

Metabolomics

Untargeted metabolomics studies reveal that the nanoarcheon *Nanoarchaeum equitans* exploits metabolites generated by its archaeal host *Ignicoccus hospitalis* as a source of energy rather than biomass production.

--Manuscript Draft--

Manuscript Number:	
Full Title:	Untargeted metabolomics studies reveal that the nanoarcheon <i>Nanoarchaeum equitans</i> exploits metabolites generated by its archaeal host <i>Ignicoccus hospitalis</i> as a source of energy rather than biomass production.
Article Type:	Original Article
Keywords:	LC-MS; NMR; Metabolomics; <i>Ignicoccus hospitalis</i> ; <i>Nanoarchaeum equitans</i> ; hyperthermophilic Archaea; interspecies interactions; metabolic pathway analysis
Corresponding Author:	Valerie Copie, Ph.D. Montana State University Bozeman, Montana UNITED STATES
Corresponding Author Secondary Information:	
Corresponding Author's Institution:	Montana State University
Corresponding Author's Secondary Institution:	
First Author:	Timothy Hamerly, B.S
First Author Secondary Information:	
Order of Authors:	Timothy Hamerly, B.S Michelle Tigges, B.S Brian P. Tripet, Ph.D. Richard J Giannone, Ph.D. Louie Wurch, Ph.D. Robert L. Hettich, Ph.D. Mircea Podar, Ph.D. Valerie Copie, Ph.D. Brian Bothner, Ph.D.
Order of Authors Secondary Information:	
Abstract:	Interactions between species are the basis of microbial community formation and infectious diseases. Systems biology now presents an opportunity for complex models describing such interactions to be constructed, leading to better understanding of disease states and communities. However, before complex interactions between organisms can be tackled, the metabolic and energetic implications of simplified real-world interactions must be worked out. To address this issue, untargeted metabolomics and proteomics measurements have been used to characterize the molecular level interactions between two hyperthermophilic species, both of which have reduced genomes. In this study, metabolic changes and transfer of metabolites between <i>Ignicoccus hospitalis</i> and <i>Nanoarchaeum equitans</i> have been investigated using integrated LC-MS and NMR metabolomics. The study of the archaeal system <i>I. hospitalis</i> - <i>N. equitans</i> is challenging, as no genetic tools are available and the mechanisms by which they interact are unknown. Together with information about relative enzyme levels obtained from shotgun proteomics, the metabolomics data have provided useful insights into metabolic pathways and cellular networks of <i>I. hospitalis</i> that are affected by the presence of <i>N. equitans</i> , including arginine, isoleucine, and CTP biosynthesis. On the organismal level, our data indicate that <i>N. equitans</i> imposes

a metabolic energy tax on *I. hospitalis*. This finding is based on *N. equitans*'s consumption of a significant fraction of the metabolite pool in *I. hospitalis* that cannot solely be attributed to increased biomass production for *N. equitans*. Combining LC-MS and NMR metabolomics datasets improved coverage of the metabolome and enhanced the identification and quantitation of cellular metabolites.

1
2
3
4 Untargeted metabolomics studies reveal that the nanoarcheon *Nanoarchaeum*
5
6
7 *equitans* exploits metabolites generated by its archaeal host *Ignicoccus hospitalis*
8
9
10 as a source of energy rather than biomass production
11
12
13
14

15 Timothy Hamerly^{1ζ}, Michelle Tigges^{1ζ}, Brian P. Tripet^{1ζ}, Richard J. Giannone³, Louie Wurch^{3,4},
16
17 Robert L. Hettich³, Mircea Podar^{3,4}, Valerie Copié^{1,2*}, and Brian Bothner^{1,2*}
18
19
20
21
22

23 ¹ Department of Chemistry and Biochemistry, Montana State University, Bozeman, MT 59717
24

25 ² Thermal Biology Institute, Montana State University, Bozeman, MT 59717
26

27 ³ Oak Ridge National Laboratory, Oak Ridge, TN 37831
28

29 ⁴Department of Microbiology, University of Tennessee, Knoxville, TN 37996
30
31
32
33
34

35 ζ. denotes that all three authors contributed equally to this work
36

37
38 * Denotes corresponding authors
39
40
41
42

43 Correspondence should be addressed to:

44
45 Drs. Brian Bothner and Valérie Copié
46

47
48 Montana State University
49

50
51 Chemistry & Biochemistry Department, CBB 103
52

53
54 Bozeman, MT 59717
55

56
57 Phone: (406)-994-5270 and (406)-994-7244
58

59
60 Email: bbothner@chemistry.montana.edu and vcopie@chemistry.montana.edu
61
62
63
64
65

1
2
3
4 Abbreviated Title: LC-MS and NMR metabolomics profiling of the *Ignicoccus hospitalis* –
5
6 *Nanoarchaeum equitans* archaeal system
7
8
9

10
11 Acknowledgment of financial support.
12

13
14 This research was supported by a grant from the U.S. Department of Energy, Office of
15
16 Biological and Environmental Research (DE-SC0006654). The NMR experiments were recorded at
17
18 Montana State University on a DRX600 Bruker solution NMR spectrometer, purchased in part with funds
19
20 from the NIH Shared Instrumentation Grant (SIG) (Grant Number 1S10-RR13878-01), and recently
21
22 upgraded to an AVANCE III console and cryogenically cooled TCI probe (Grant Number 1S10-
23
24 RR026659-01). The mass spectrometry facility at MSU receives funding from the Murdock Charitable
25
26 Trust and NIH 5P20RR02437 of the Cobre program. We thank Dr. Harald Huber (University of
27
28 Regensburg, Germany) for providing a bioreactor sample of *I. hospitalis-N. equitans* used for initial
29
30 methods development.
31
32
33
34
35
36
37
38
39
40
41
42
43
44
45
46
47
48
49
50
51
52
53
54
55
56
57
58
59
60
61
62
63
64
65

1
2
3
4 **Abstract**
5

6 **Interactions between species are the basis of microbial community formation and infectious**
7 **diseases. Systems biology now presents an opportunity for complex models describing such**
8 **interactions to be constructed, leading to better understanding of disease states and**
9 **communities. However, before complex interactions between organisms can be tackled, the**
10 **metabolic and energetic implications of simplified real-world interactions must be worked**
11 **out. To address this issue, untargeted metabolomics and proteomics measurements have**
12 **been used to characterize the molecular level interactions between two hyperthermophilic**
13 **species, both of which have reduced genomes. In this study, metabolic changes and**
14 **transfer of metabolites between *Ignicoccus hospitalis* and *Nanoarchaeum equitans* have been**
15 **investigated using integrated LC-MS and NMR metabolomics. The study of the archaeal**
16 **system *I. hospitalis* – *N. equitans* is challenging, as no genetic tools are available and the**
17 **mechanisms by which they interact are unknown. Together with information about relative**
18 **enzyme levels obtained from shotgun proteomics, the metabolomics data have provided**
19 **useful insights into metabolic pathways and cellular networks of *I. hospitalis* that are**
20 **affected by the presence of *N. equitans*, including arginine, isoleucine, and CTP**
21 **biosynthesis. On the organismal level, our data indicate that *N. equitans* imposes a**
22 **metabolic energy tax on *I. hospitalis*. This finding is based on *N. equitans*'s consumption of**
23 **a significant fraction of the metabolite pool in *I. hospitalis* that cannot solely be attributed**
24 **to increased biomass production for *N. equitans*. Combining LC-MS and NMR**
25 **metabolomics datasets improved coverage of the metabolome and enhanced the**
26 **identification and quantitation of cellular metabolites.**
27
28
29
30
31
32
33
34
35
36
37
38
39
40
41
42
43
44
45
46
47
48
49
50
51
52
53
54
55
56
57
58
59
60
61
62
63
64
65

1
2
3
4
5
6
7
8
9
10
11
12
13
14
15
16
17
18
19
20
21
22
23
24
25
26
27
28
29
30
31
32
33
34
35
36
37
38
39
40
41
42
43
44
45
46
47
48
49
50
51
52
53
54
55
56
57
58
59
60
61
62
63
64
65

Key words:

LC-MS; NMR; metabolomics; *Ignicoccus hospitalis*; *Nanoarchaeum equitans*; hyperthermophilic Archaea; interspecies interactions; metabolic pathway analysis

1
2
3
4 **Introduction**
5

6 In the environment, microbes do not live in isolation, rather they are constantly
7
8 responding to the presence of other species, adapting their metabolic needs and resources to
9
10 optimize growth and survival among species that share similar ecological niches. Microbial
11
12 communities depend on specific and complex mechanisms of interspecies interactions and
13
14 communications, forming complex interspecies networks ranging from mutualism to symbiosis
15
16 or parasitism. Such interspecies relationships impact the role of keystone species in an ecological
17
18 community, play a major role in energy and elemental cycles, and form the foundation of host-
19
20 pathogen interactions. Despite a long history of research focused on better understanding of the
21
22 molecular mechanisms underlying host-microbe interactions, and the growing interest in
23
24 identifying microbial metacommunities, fundamental processes of interspecies recognition,
25
26 interactions, and communication remain unclear. In particular, little is known about the
27
28 biochemical processes by which mutualism and syntrophy (i.e. metabolic interdependence)
29
30 impact microbial genome evolution, and how metabolism and energetic coupling between
31
32 species affect host-microbe homeostasis and their responses to environmental factors. Such a
33
34 lack of fundamental knowledge is most prevalent for organisms from the Archaeal domain of
35
36 life, such as *Ignicoccus hospitalis* and *Nanoarchaeum equitans*, which engage in one of the
37
38 simplest symbiotic/parasitic systems known (Jahn *et al.*, 2008; Junglas *et al.*, 2008; Podar *et al.*,
39
40 2008).
41
42
43
44
45
46
47
48
49

50 The reduced genome complexity of *I. hospitalis* and *N. equitans* makes this a tractable
51
52 model for study of fundamental cellular, genomic, and metabolic principles guiding inter-species
53
54 interactions, as the genomes of both organisms have been sequenced, a metabolic map of the
55
56 *Ignicoccus-Nanoarchaeum* system has been reconstructed, and some of the biochemical pathways
57
58
59
60
61
62
63
64
65

1
2
3
4 and cellular complexes have been experimentally validated (Huber *et al.*, 2008; Huber *et al.*,
5
6 2003; Jahn *et al.*, 2007; Jahn *et al.*, 2004; Küper *et al.*, 2010; Podar *et al.*, 2008; Waters *et al.*,
7
8 2003). *Ignicoccus* represents a genus of marine hyperthermophilic, chemolithoautotrophic
9
10 Archaea, classified to the order Desulfurococcales (Huber *et al.*, 2000). These organisms reduce
11
12 elemental sulfur with hydrogen as a source of energy and carbon dioxide as the sole carbon
13
14 source (Jahn *et al.*, 2007). *Ignicoccus hospitalis* possesses one of the smallest genomes of any
15
16 free living organism, having less than 1500 genes (Podar *et al.*, 2008). One species of this genus
17
18 (*Ignicoccus hospitalis*) has been shown to act as a host for one of the smallest organisms known,
19
20 *Nanoarchaeum equitans*, which encodes approximately 550 proteins, lacks many of the genes
21
22 requires for energy production, and depends exclusively on *Ignicoccus* for survival (Giannone *et*
23
24 *al.*, 2011; Huber *et al.*, 2002; Huber *et al.*, 2003; Paper *et al.*, 2007). *N. equitans* is a member of
25
26 the proposed phylum *Nanoarchaeota*, and currently the only cultivated organism from that group
27
28 of Archaea (Huber *et al.*, 2000; Huber *et al.*, 2002).

29
30
31
32
33
34
35
36 Early investigations into the protein composition of *N. equitans* revealed that it is
37
38 comprised of a very minimal proteome with important bioenergetic proteins and protein
39
40 complexes missing or incomplete (Giannone *et al.*, 2011; Waters *et al.*, 2003). In addition, *N.*
41
42 *equitans* is unable to synthesize many metabolites and lipids on its own, and relies on essential
43
44 cellular nutrients and metabolic components that are provided via interaction and cell-cell
45
46 contact with *I. hospitalis* (Burghardt *et al.*, 2009; Huber *et al.*, 2012; Jahn *et al.*, 2004).
47
48
49

50
51 Despite these observations, it remains to be established whether *N. equitans* acts as a
52
53 parasite or provides any symbiotic advantages to *I. hospitalis*, as the latter does not seem to
54
55 benefit or suffer when grown in co-culture with *N. equitans* (Burghardt *et al.*, 2009; Giannone *et*
56
57 *al.*, 2011; Godde, 2012; Huber *et al.*, 2012; Jahn *et al.*, 2008, 2004; Junglas *et al.*, 2008).
58
59
60
61
62
63
64
65

1
2
3
4 In order to better understand the foundational biochemistry and metabolic networks
5
6 regulating *I. hospitalis* – *N. equitans* interspecies interactions, we have undertaken an untargeted
7
8 mass spectrometry (MS) and nuclear magnetic resonance (NMR) based metabolomics study of
9
10 this archaeal host-microbe model system. Utilization of both NMR and MS have enabled us to
11
12 take advantage of the complementarity of the two techniques for metabolomics analysis, and to
13
14 establish distinct metabolite profiles of *I. hospitalis* alone and when grown in co-culture with *N.*
15
16 *equitans*. The metabolomics data thus acquired have been integrated with published genomics
17
18 and proteomics information using Pathway Tools, to generate a multilevel model of cellular
19
20 processes (genes, proteins, metabolites) and metabolic networks that regulate *I. hospitalis* and *N.*
21
22 *equitans* interactions (Karp & Paley, 1996; Karp *et al.*, 2005, 2010; Karp, et al., 2002; Paley et
23
24 al., 2012). Results from the global analysis of multi “omics” data suggest that *N. equitans*
25
26 imposes a metabolic energy tax on *I. hospitalis*, while still allowing both organisms to live.
27
28
29
30
31
32
33
34
35

36 **Methods and Materials**

37 *Materials*

38
39
40
41 All solvents from metabolite extraction and LC-MS analysis were purchased in HPLC
42
43 grade; water from Avantor (Center Valley, PA) and methanol and acetonitrile from EMD
44
45 Chemicals Inc. (Gibbstown, NJ). Formic acid (98% GR ACS) for use as an ion pairing agent was
46
47 purchased from EMD Chemicals Inc. (Gibbstown, NJ). DSS (4,4-dimethyl-4-silapentane-1-
48
49 sulfonic acid) used for NMR spectral reference and metabolite quantification was purchased
50
51 from Sigma. All solvents were used as supplied without further purification.
52
53
54
55
56
57
58
59
60
61
62
63
64
65

1
2
3
4 *Cell Culturing*
5

6 *I. hospitalis* and *I. hospitalis* – *N. equitans* were cultured for 24 hours in 1 liter bottles
7
8 containing 250 ml 0.5X SME medium, sulfur (10g/l) and a H₂-CO₂ (80-20%) gas phase (15 psi),
9
10 at 85 °C, as described previously (Jahn *et al.*, 2008). Prior to harvesting, the cultures were cooled
11
12 to room temperature, chilled on ice and the cells were collected by centrifugation (8000 xg for 20
13
14 minutes). The cell pellets were washed with cold anaerobic 0.5X SME medium, aliquoted in
15
16 small tubes, and flash frozen with liquid nitrogen under N₂ gas, and stored at -80 °C.
17
18
19
20
21
22

23 *Metabolite Extraction*
24

25
26 Intracellular metabolites from *I. hospitalis* and *I. hospitalis*-*N. equitans* co-cultures for
27
28 LC-MS and NMR analysis were extracted using a 50% aqueous (v/v) MeOH extraction,
29
30 modified from a previously published protocol (Heinemann *et al.*, 2014). Briefly, frozen cell
31
32 pellets weighing 50 mg for LC-MS analysis and 115 mg for NMR analysis, were re-suspended in
33
34 300 µL of 50% MeOH (v/v), vortexed for 30 seconds, and lysed by sonication for 5 minutes on
35
36 ice. The resulting samples were then incubated for 1 hour at -20 °C to allow diffusion of
37
38 metabolites into the bulk liquid. Following this step, cell debris was pelleted by centrifugation
39
40 for 15 minutes at 20,000 ×g and supernatant was collected. Cell debris was then washed with an
41
42 additional volume of 50% MeOH (v/v), vortexed for 30 seconds, centrifuged, and supernatant
43
44 pooled. Proteins were precipitated using 5:1 dilution with cold acetone, left overnight at -80 °C,
45
46 and centrifuged. The resulting supernatant was collected and dried via vacuum speed
47
48 concentration, and stored at -80 °C. For LC-MS analysis, metabolite extracts were re-suspended
49
50 in 50% MeOH.
51
52
53
54
55
56
57
58
59
60
61
62
63
64
65

1
2
3
4 *LC-MS Based Metabolomic Analysis*
5

6 For reverse phase analysis, a Kinetex 1.7 μm C18 150 mm x 2.1 mm column
7
8 (Phenomenex, Torrance, CA) kept at 50 $^{\circ}\text{C}$ was used for LC separation with a flow rate of 600
9 $\mu\text{L min}^{-1}$. Solvent A consisted of 0.1% formic acid in water, while solvent B was 0.1% formic
10 acid in acetonitrile. The elution gradient consisted of 2% solvent B for 2 minutes (with the first
11 two minutes going to waste to avoid contaminating the source with excess salt), to 95% solvent
12 B over 24 minutes, held at 95% for 2 minutes, and then returned to 2% for 2 minutes, with a total
13 run time of 30 minutes using an Agilent 1290 UPLC (Agilent, Santa Clara, CA) system
14 connected to an Agilent 6538 Q-TOF Mass Spectrometer (Agilent, Santa Clara, CA).
15
16
17
18
19
20
21
22
23
24
25

26 For normal phase analysis, a Cogent Diamond Hydride HILIC 150 mm x 2.1 mm column
27 (MicroSolv, Eatontown, NJ) was used for LC separation with a flow rate of 600 $\mu\text{L min}^{-1}$.
28
29 Solvent A consisted of 0.1% formic acid in water, while solvent B consisted of 0.1% formic acid
30 in acetonitrile. The elution gradient consisted of 95% solvent B for 2 minutes (with the first
31 minute going to waste to avoid contaminating the source with excess salt), to 50% solvent B over
32 24 minutes, held at 50% for 2 minutes, and then returned to 95% for 2 minutes, with a total run
33 time of 30 minutes using an Agilent 1290 UPLC (Agilent, Santa Clara, CA) system connected to
34 an Agilent 6538 Q-TOF Mass Spectrometer (Agilent, Santa Clara, CA).
35
36
37
38
39
40
41
42
43
44
45

46 Mass spectrometry analysis was conducted in positive ion mode, with a cone voltage of
47 3500V and a fragmentor voltage of 120V. Drying gas temperature was 350 $^{\circ}\text{C}$ with a flow of 12
48 L min^{-1} and the nebulizer was set to 60 psig. Spectra were collected at a rate of 2.52 per second
49 with a mass range of 50 to 1000 m/z. The mass analyzer resolution was 18,000 and post
50 calibration tests had a mass accuracy of approximately one ppm.
51
52
53
54
55
56
57
58
59
60
61
62
63
64
65

1
2
3
4 *LC-MS Data Processing and Analysis*
5

6 Data files from the LC-MS were converted to .MZxml format using the Masshunter
7
8 Qualitative software provided with Agilent instruments (Agilent, Santa Clara, CA). Analysis of
9
10 LC-MS data was done using the software package MZmine (version 2.10). Procedures, together
11
12 with parameters used for the alignment of features and identification in MZmine, were as
13
14 follows: LC-MS files were imported into MZmine, followed by data set filtering to remove the
15
16 first minute of elution data for HILIC analysis, and the first two minutes of elution data for RP
17
18 analysis. A minimum intensity cutoff of 5000 and a minimum elution time window of 0.1
19
20 minutes were used to create molecular feature lists. Lists included retention time (R/T) adjusted
21
22 with a tolerance of 0.2 minutes or less. These R/T-adjusted lists were then aligned into one mass
23
24 list, and then gap-filled to add missing peaks not detected in all runs with an m/z tolerance of
25
26 15.0 ppm. Identification of compounds was based on annotated pathways in Biocyc, or standard
27
28 compounds based on R/T and m/z was done on these finalized lists with an m/z tolerance of 30
29
30 ppm and for the standards a retention time tolerance of 0.25 minutes (Karp *et al.*, 2005, 2002).
31
32 Metabolite identities were each manual annotated to ensure strong matches, while no tandem
33
34 mass spectrometry was done to further confirm metabolite ID. Lists of aligned and R/T adjusted
35
36 molecular features were analyzed using principal component analysis (PCA) using the XLSTAT
37
38 software package (Addinsoft 2013).
39
40
41
42
43
44
45
46
47
48
49

50 *NMR Based Metabolomic Analysis and Data Processing*
51

52 For ¹H 1D NMR, duplicate metabolite samples were resuspended in 200 μL of
53
54 NMR buffer (10mM NaH₂PO₄/ Na₂HPO₄ containing 0.25 mM 4,4-dimethyl-4-silapentane-1-
55
56 sulfonic acid (DSS) in 100% D₂O, pH 7) and transferred to a 5 mm Shigemi high salt NMR tube
57
58
59
60
61
62
63
64
65

1
2
3
4 (Shigemi Inc.). ^1H NMR spectra were acquired at 298K (25 $^{\circ}$ C) on a Bruker 600-MHz (^1H Larmor
5
6 frequency) AVANCE III solution NMR spectrometer equipped with a SampleJetTM automatic
7
8 sample loading system, a 5 mm triple resonance (^1H , ^{15}N , ^{13}C) liquid helium-cooled TCI probe
9
10 (cryoprobeTM), and TopspinTM software (Bruker version 3.2). One-dimensional ^1H NOESY
11
12 experiments were performed using the Bruker supplied noesypr1d pulse sequence with 256
13
14 scans, ^1H spectral window of 9600 Hz. FIDS were collected in 32K data points, with a dwell
15
16 time interval of 52 usec amounting to an acquisition time of ~ 1.7 sec, using a 2 second
17
18 relaxation recovery delay between acquisitions, and a NOESY mixing time period of 50 msec.
19
20 Pulse sequence settings were based on standard recommendations by the Chenomx guide for
21
22 recording 1D ^1H NMR spectra of small molecules and for quantitation of metabolites.
23
24
25
26
27

28
29 Spectral processing and analysis was performed using the Chenomx NMR software
30
31 (version 7.6) (Chenomx Inc., Edmonton, AB, Canada). For each sample, NMR spectra were
32
33 phased, baseline corrected, and a line broadening function of 0.5 Hz was applied, following
34
35 recommended Chenomx protocols and previously reported metabolomics analysis methods (Sun
36
37 *et al.*, 2012; Tredwell *et al.*, 2011; Weljie *et al.*, 2006; Wu *et al.*, 2010). For metabolite
38
39 identification, the Chenomx small molecule library for 600-MHz (^1H Larmor frequency)
40
41 magnetic field strength NMR was used, and NMR spectral patterns were fitted for each sample
42
43 independently. The internal DSS standard was used for quantitation of identified metabolites.
44
45
46
47
48
49

50 *Pathway Tools Analysis of Overlaid Metabolomic and Proteomic Datasets*

51
52
53 Using the Pathway Tools v17.5 software (SRI International), NMR and LC-MS
54
55 metabolite identities and abundances were overlaid with previously published proteomics
56
57 datasets for *I. hospitalis* only cultures and *I. hospitalis* – *N. equitans* co-cultures (Giannone *et al.*
58
59
60
61
62
63
64
65

1
2
3
4 2011a; Karp & Paley 1996; Karp et al. 2005, 2010, 2002; Paley et al. 2012). Metabolite identities
5
6 and their associated fold changes were overlaid onto the IHOS453591 Cyc version 17.0
7
8 database, which is available directly from the Biocyc webservers (Karp et al. 2005, 2002). The
9
10 constructed pathway tools database was further curated and adjusted based on analysis of
11
12 published literature on *I. hospitalis* and *N. equitans*.
13
14

15 16 17 18 19 *Firefly Luciferase Assay for Quantitation of ATP*

20
21 Determination of ATP concentrations in both cultures was carried out using the BacTiter-
22
23 Glo Firefly Luciferase Assay (Promega, Madison, WI) following the protocol included with the
24
25 kit (Promega Corporation 2012). Briefly, BacTiter-Glo buffer and BacTiter-Glo substrate were
26
27 equilibrated to room temperature. Substrate was then re-suspended in 10 mL buffer with gentle
28
29 vortexing to form the BacTiter-Glo reagent. To perform the ATP measurements, 6.5 mg of *I.*
30
31 *hospitalis* and *I. hospitalis* – *N. equitans* co-culture cell pellets were re-suspended in 100 μ L of
32
33 H₂O, and placed into a white 96-well plate. Cells in solution were allowed to equilibrate to room
34
35 temperature, and then an equal volume (100 μ L) of BacTiter-Glo reagent was added to each well
36
37 with cells, as well as to a well containing 100 μ L of H₂O only to serve as a blank. A standard
38
39 curve of ATP concentrations was generated from 1 μ M to 10 pM from a 1 μ M stock solution and
40
41 mixed with BacTiter-Glo reagent and also placed in the same white 96-well plate. The plate was
42
43 placed on an orbital shaker (Thermoscientific) for five minutes to assist with cell lysis.
44
45
46 Luminescence readings for the assay were recorded on a Fluoroskan Ascent FL Microplate
47
48 Luminometer (Thermo Fisher Scientific Inc., Waltham, MA) and data processing of data was
49
50
51
52
53
54
55
56
57
58
59
60
61
62
63
64
65 accomplished using the Ascent Software.

Results and Discussion

LC-MS Based Metabolomics Analysis

Metabolite extracts of *I. hospitalis* cells grown alone and in co-culture with *N. equitans* were analyzed using liquid chromatography-mass spectrometry (LC-MS). Three independent biological replicates were used for each type of cell culture. Differential analysis based on molecular feature intensity was used to compare sample groups. Figure 1A presents a cloud plot of reverse phase LC-MS metabolite data from *I. hospitalis* alone and in co-culture with *N. equitans*. Red circles indicate features that are in greater abundance when *I. hospitalis* is grown alone, while green circles indicates features that are in greater abundance in the *I. hospitalis-N. equitans* co-culture. The size of the circle indicates fold change between cultures and the shade of each color indicates *p*-value, where larger, darker circles indicate greater fold change and more significant *p*-values. A number of differences between cultures were observed from these data. Greater than 3000 molecular features were detected between the 6 samples, with approximately 100 features being significantly distinct between groups (i.e. exhibiting fold changes greater than 1.5 and a *p*-value less than 0.01). The vast majority of metabolite changes corresponded to decreases in metabolite abundance in the *I. hospitalis-N. equitans* co-cultures. Figure 1B displays the results from a principal component analysis (PCA) of molecular features identified from *I. hospitalis* and co-culture samples (in triplicate). This figure indicates that *I. hospitalis* only cultures and *I. hospitalis – N. equitans* co-cultures clearly separate from each other along the first principal component (PC1) axis, with PC1 and PC2 accounting to ~ 71% of the variance between cultures. A Venn diagram of molecular features found exclusively in *I. hospitalis* or in co-culture samples, as well as the number of molecular features found in both sets of samples, is shown in Figure 1C.

1
2
3
4 As a large number of molecular features were observed, data reduction was undertaken to
5
6 tease out putative biologically interesting metabolites from the LC-MS metabolomics
7
8 experiments. Two main data reduction strategies were conducted: First, a small in-house
9
10 database of prominent and microbial-relevant compounds was created and annotated using
11
12 retention times and masses (m/z ratios) from the large set of LC-MS spectra. This database
13
14 enabled positive identification of compounds based on both accurate mass and retention time
15
16 characteristics. As establishing an exhaustive library of standards for all putative compounds is
17
18 not practical, additional data reduction was conducted to further mine the data for biologically
19
20 interesting compounds. Specifically, biologically relevant metabolites to the *I. hospitalis* – *N.*
21
22 *equitans* system were highlighted by matching molecular masses within a 20 ppm mass error
23
24 range to a list of expected compounds based on curated genome annotation via the Biocyc
25
26 pathway tools software (Karp et al. 2010).
27
28
29
30
31
32

33 Metabolites identified as a result of this LC-MS analysis are displayed in first four
34
35 columns of Table 1. A fold change was calculated for each metabolite identified, where a
36
37 positive number denotes a higher concentration when *I. hospitalis* is grown alone, and a negative
38
39 fold change indicates a higher concentration in the *I. hospitalis* – *N. equitans* co-culture. A total
40
41 of 39 compounds were putatively identified from the LC-MS analysis by matching molecular
42
43 features with predicted compounds based on genome annotation, or by matching features to
44
45 standards based on retention time and accurate mass measurements. Although a small number,
46
47 the identities were strong matches and expected to be present in cells (such as amino acids, or
48
49 energy molecules like adenosine monophosphate involved in energy production). Of the 39
50
51 putatively identified molecules, 21 were confirmed by mass accuracy and retention time of
52
53 standard molecules. Interestingly, several sugars were identified and confirmed by standards,
54
55
56
57
58
59
60
61
62
63
64
65

1
2
3
4 which do not appear to be annotated in any known metabolic pathways of *I. hospitalis* or *N.*
5
6
7 *equitans* and included maltotriose and stachyose.
8
9

10 11 *NMR Based Metabolomics Analysis* 12 13

14 Nuclear magnetic resonance (NMR) metabolomics analysis is highly complementary to
15
16 metabolite profiling by LC-MS. In addition to helping confirm putative metabolite identities
17
18 from LC-MS, NMR yields quantitative information on metabolite concentrations and is able to
19
20 detect molecules that may not be observable by LC-MS. Figure 2 displays 1D ¹H NMR spectra
21
22 obtained from metabolite extracts of *I. hospitalis* grown alone (Figure 2A), and in co-culture
23
24 with *N. equitans* (Figure 2B). A total of 55 metabolites were identified from analysis of the 1D
25
26 ¹H NMR spectra of *I. hospitalis* and *I. hospitalis* – *N. equitans* cultures, by matching NMR
27
28 spectral patterns to reference metabolite spectra of the Chenomx database (Chenomx NMR Suite
29
30 7.0, 2010; Wishart, 2008). Eighteen of the 20 common amino acids, energy molecules like ADP,
31
32 and nucleotides were identified by NMR and found to be higher in concentration in *I. hospitalis*
33
34 grown alone compared to *I. hospitalis* grown in co-culture with *N. equitans*. Columns four and
35
36 five of Table 1 list metabolites identified by NMR. As with the LC-MS metabolite data, a
37
38 positive fold change indicates higher concentration when *I. hospitalis* is grown alone, and a
39
40 negative fold change indicates higher concentration when *I. hospitalis* is grown in co-culture
41
42 with *N. equitans*. Star and pound symbols were also used to denote metabolites found in one but
43
44 not the other type of cultures, similar to what has been used for the LC-MS data.
45
46
47
48
49
50
51
52

53 In addition to amino acids and energy molecules like ADP identified by NMR as being
54
55 present at higher concentrations when *I. hospitalis* is grown alone, the overall concentration of
56
57 all metabolites, as assessed by the overall integrated intensity of all NMR signals in the 1D ¹H
58
59
60
61
62

1
2
3
4 spectra, is almost five times greater when *I. hospitalis* is grown alone. This suggests that the
5
6 intracellular pool of small molecule metabolites present when *I. hospitalis* is cultured by itself is
7
8 depleted when *I. hospitalis* is grown together with *N. equitans* (Figure 2). Based on internal
9
10 NMR and LC-MS standards used to normalize total signal intensities for metabolites, nearly all
11
12 of the molecular features and metabolites showed a decrease in abundance in the co-culture
13
14 samples.
15
16
17
18
19
20

21 *LC-MS and NMR Metabolic Profiling*

22

23
24 Overall, the LC-MS and NMR data proved highly complementary. While the LC-MS
25
26 based approach was able to identify metabolites present at low concentrations, metabolite
27
28 profiling by NMR resulted in the confident identification and accurate concentrations of each
29
30 NMR identified metabolite. A total of 15 compounds were identified by both LC-MS and NMR,
31
32 with comparable fold changes measured by both methods for almost all compounds of interest,
33
34 except phenylalanine. There were also cases where one method could not obtain a reliable fold
35
36 difference between *I. hospitalis* alone and the co-culture, due to low metabolite signal intensity
37
38 or overlapping spectral peaks, but the complementary method could (see L-Proline or L-
39
40 Pyroglumate for examples). In these cases, the ability to confirm the presence of a molecule by
41
42 both methods was extremely helpful. In combination, nearly 70 metabolites were identified
43
44 between the two techniques, clearly demonstrating the power of using LC-MS and NMR
45
46 together for comprehensive profiling of metabolites.
47
48
49
50
51
52
53
54

55 *Metabolic Pathway Analysis of LC-MS and NMR Metabolomics Data*

56
57
58
59
60
61
62
63
64
65

1
2
3
4 The LC-MS and NMR metabolomics data, and resulting metabolic profiles observed,
5
6 were subsequently analyzed in the context of what is known about the metabolism of *I. hospitalis*
7
8 and *N. equitans*, and current understanding of cellular events regulating *I. hospitalis* – *N.*
9
10 *equitans* host interactions, using annotated genome-based network maps. Using the Pathway
11
12 Tools program, proteins and metabolites identified were mapped onto known biochemical
13
14 pathways of *I. hospitalis* and *N. equitans*, providing a global, system-wide analysis of metabolic
15
16 networks that may be guiding cellular interactions between these two organisms. This resulting
17
18 map of proteomic and metabolomic datasets highlights several pathways annotated by enzymes
19
20 and metabolites that have been identified in the proteomics and metabolomics studies. This
21
22 includes arginine biosynthesis, isoleucine biosynthesis, and CTP/UTP biosynthesis and nutrient
23
24 recycling (Figure 3). Although other amino acid pathways are altered by the presence of *N.*
25
26 *equitans*, there is a strong correlation between proteomic and metabolomics data for arginine and
27
28 isoleucine biosynthesis that warrants further analysis.
29
30
31
32
33
34

35
36 A precursor to arginine synthesis is the amino acid ornithine, which undergoes
37
38 condensation with carbamoyl-phosphate to form citrulline, as depicted in Figure 3A. Citrulline is
39
40 then converted to arginine via action of arginosuccinate synthase and lyase enzymes (Figure 3A).
41
42 Analysis of this pathway reveals that enzymes involved in the synthesis of ornithine are down-
43
44 regulated when *N. equitans* is grown in culture with *I. hospitalis*, indicating that little ornithine
45
46 accumulates in *I. hospitalis*- *N. equitans* co-cultures compared to *I. hospitalis* only cultures.
47
48 However, a substantial build-up of intracellular ornithine is observed in *I. hospitalis* only
49
50 cultures, which disappears when *N. equitans* is present. Nearly 16 times more ornithine can be
51
52 measured in *I. hospitalis* only cultures when using comparable cell mass for metabolite
53
54 extractions. This indicates that when *N. equitans* is present, the synthesis of arginine is largely
55
56
57
58
59
60
61
62
63
64
65

1
2
3
4 accomplished through the consumption of available ornithine, and not by up-regulating
5
6 metabolic enzymes needed to synthesize more ornithine. It should also be noted that there are no
7
8 other annotated pathways in *I. hospitalis* and *N. equitans* for which ornithine is a substrate,
9
10 strongly suggesting that ornithine is used exclusively for arginine biosynthesis. This also
11
12 indicates that *N. equitans* is using available biomolecules from *I. hospitalis* to produce arginine
13
14 in as few steps as possible, presumably to conserve energy.
15
16
17

18
19 The pathway for isoleucine production (Figure 3B) appears to shift in the opposite
20
21 direction to what is expected if one considers metabolic needs for isoleucine based on protein
22
23 biomass production. The percentage of the proteome comprised of isoleucine in *I. hospitalis* and
24
25 *N. equitans* are 4.9% and 10.5% respectively. This would suggest that, assuming one of every
26
27 protein is synthesized *de novo* by each organism, *N. equitans* would have a greater metabolic
28
29 need for isoleucine than *I. hospitalis*. However, enzymes involved in the synthesis of isoleucine
30
31 are all down-regulated when *N. equitans* is grown in co-culture with *I. hospitalis*, suggesting that
32
33 isoleucine biosynthesis is decreased when the two organisms are grown together.
34
35
36
37

38
39 Other amino acids appear to play a key role in modulated metabolic networks between *I.*
40
41 *hospitalis* and *N. equitans*. Overall, the depletion of amino acids when *N. equitans* is present in
42
43 co-culture with *I. hospitalis*, and the decreased abundance of enzymes involved in biosynthetic
44
45 pathways such as isoleucine which is needed for protein production in *N. equitans*, suggests that
46
47 amino acids are being catabolized for energy production purposes, and not used significantly in
48
49 protein biosynthesis and biomass production. This is further evidenced given that only a small
50
51 amount of the cell mass in the co-culture is actually contributed by *N. equitans*. With an average
52
53 of two *N. equitans* per *I. hospitalis*, and a cell volume of just 1% of *I. hospitalis* per *N. equitans*,
54
55 roughly 2% of the overall cell mass in the co-culture is *N. equitans*. Although the actual protein
56
57
58
59
60
61
62
63
64
65

1
2
3
4 concentration is not known, using the concentration of other single cell organisms of 100
5
6 mg/mL, the amount of protein which may be assigned to *N. equitans* accounts for less than half
7
8 of the total consumed amino acids based on concentrations established by NMR (Moran,
9
10
11
12 Phillips, & Milo 2010).

13
14 A final metabolic pathway of particular significance, as assessed by the convergence of
15
16 proteomic and metabolomics data, is the biosynthesis cytidine triphosphate (CTP) (Figure 3C).
17
18 This pathway is of interest because it is an energy intensive process involving the expenditure of
19
20 several equivalent of adenosine triphosphate (ATP), when the upstream synthesis of uridine
21
22 monophosphate (UMP) is included. Many of the proteins and metabolites in this pathway are not
23
24 only detected but showed significantly lower abundance in the co-culture samples. Moreover,
25
26 the end product CTP is essential for the synthesis of the archaeal lipid, archaeol (Boucher *et al.*,
27
28 2004). A key point of interest is the high energy cost to produce CTP. The final three steps in
29
30 the biosynthesis of CTP each consumes one ATP equivalent, meaning that the synthesis of one
31
32 high energy CTP requires the consumption of three high energy ATP equivalents. Interestingly,
33
34 cytidine monophosphate was found by LC-MS to be at a higher concentration in *I. hospitalis*
35
36 grown alone. From the observed depletion of CMP levels in the *I. hospitalis* – *N equitans* co-
37
38 cultures, we infer that CMP is used to produce more CTP in the *I. hospitalis-N equitans* co-
39
40 cultures, perhaps to be used for the biosynthesis of membrane lipid archaeol, where CTP links to
41
42 the glycerol backbone of archaeol to form CDP-archaeol (Boucher *et al.*, 2004). The resulting
43
44 lipid is then saturated by action of the enzyme geranyl-geranyl reductase, generating the active
45
46 form of the lipid to be incorporated into cellular membranes (Boucher *et al.*, 2004). These
47
48 observations are consistent with *N. equitans* requirements to consume ATP for CTP production
49
50 as a mean to synthesize membrane lipids for growth.
51
52
53
54
55
56
57
58
59
60
61
62
63
64
65

1
2
3
4 All together, these results strongly suggest that *N. equitans* is using metabolites generated
5
6 by *I. hospitalis* as a source of energy rather than for biomass production. To further explore this
7
8 hypothesis, ATP, ADP, and AMP levels were measured in both *I. hospitalis* only and *I.*
9
10 *hospitalis-N. equitans* co-cultures. Table 1 indicates that both LC-MS and NMR were able to
11
12 identify AMP, and NMR was also able to identify ADP. Both ADP and AMP were found to be
13
14 in higher concentrations in the *I. hospitalis* only cultures. To quantify the ATP levels, a firefly
15
16 luciferase ATP assay was carried out and produced similar results: ATP was found to be in
17
18 higher concentration when *I. hospitalis* is grown without *N. equitans*. All three molecules (ATP,
19
20 ADP, and AMP) were thus lower in concentrations in the *I. hospitalis- N equitans* co-cultures,
21
22 supporting the supposition that the overall pool of intracellular metabolites of *I. hospitalis* is
23
24 consumed in the presence of *N. equitans*, and that the latter is using these molecules for energy
25
26 production. Additionally, the ratio of ADP to ATP is larger in the co-culture (104 for *I. hospitalis*
27
28 grown alone and 176 for the co-culture), indicating that in addition to having lower
29
30 concentrations of adenosine phosphates, the cells in the co-cultures experience lower energy
31
32 balance.
33
34
35
36
37
38
39

40 Results from the ATP luciferase assays clearly demonstrate that presence of *N. equitans*
41
42 in *I. hospitalis* cultures results in the expenditure of ATP. This energy may be used to produce
43
44 CTP, as suggested by the metabolic pathway analysis described above. This is also supported by
45
46 NMR metabolite profiling data which report that the nucleotide bases (specifically cytidine and
47
48 uridine) are in a higher concentration in the *I. hospitalis-N. equitans* co-cultures compared to the
49
50 *I. hospitalis* only cultures. These results provide further support for the notion that lipid
51
52 production by *I. hospitalis* relies on available CTP levels, which originate from UMP
53
54 biosynthesis as well as directly from cytidine metabolism.
55
56
57
58
59
60
61
62
63
64
65

1
2
3
4 Integration of results from proteomics and metabolomics experiments into a global scale
5
6 analysis of metabolic pathways and networks of the combined cellular potential of *I. hospitalis*
7
8 and *N. equitans* suggests that *N. equitans* exhibits parasitic function, not only consuming
9
10 metabolites for energy production but also using *I. hospitalis* to build important structural and
11
12 cellular components such as membrane lipids. Both LC-MS and NMR analyses have noted a
13
14 large decrease in the overall intracellular metabolite pool when the two organisms are grown
15
16 together, indicating that *N. equitans* stimulates the consumption of intracellular metabolites of *I.*
17
18 *hospitalis*. Further analysis of the energy status of these cells demonstrates that the presence of
19
20 *N. equitans* decreases intracellular nucleotide concentrations, and shifts the energy potential to a
21
22 lower energy state as indicated by lower ATP to ADP ratios in the *I. hospitalis* – *N. equitans* co-
23
24 cultures.
25
26
27
28
29
30
31
32

33 *Biological Significance of the LC-MS and NMR Metabolomics Data*

34

35
36 As noted above, both NMR and LC-MS metabolomics yielded a significance decrease in
37
38 abundance of nearly all metabolites. Lower amino acid concentrations in the *I. hospitalis* – *N.*
39
40 *equitans* co-cultures suggest that those metabolites are utilized by *N. equitans* for protein
41
42 biosynthesis or catabolized for energy production, or likely a combination of both. From this
43
44 standpoint, it would suggest that *N. equitans*, as a user of *I. hospitalis* metabolic resources, may
45
46 be acting more as a parasite rather than a mutualist with respect to its *I. hospitalis* host.
47
48
49

50
51 Given that the total concentration of all metabolites is greater in *I. hospitalis* alone, and
52
53 similar amounts of cells were used to extract metabolites in each sample, lower metabolite
54
55 concentrations in *I. hospitalis*-*N. equitans* co-cultures suggests that *N. equitans* is consuming
56
57 metabolites produced by *I. hospitalis* to meet its own metabolic and growth needs. However the
58
59
60
61
62
63
64
65

1
2
3
4 question remains as to whether *I. hospitalis* could benefit from interactions with *N. equitans*, as
5
6 many of the metabolic networks for these two organisms remain to be deciphered. For example,
7
8 identification of maltotriose and stachyose as significant *I. hospitalis* metabolites suggest that *I.*
9
10 *hospitalis* may be capable of more complex carbohydrate metabolism than has been anticipated.
11
12 The LC-MS data on carbohydrate intermediates suggest that glucose or other carbohydrate
13
14 storage pathways are present in *I. hospitalis* and may serve to maintain proper cellular osmotic
15
16 control.
17
18
19
20
21
22

23 **Conclusion**

24
25
26 A more complete view of the metabolome of *I. hospitalis* and *N. equitans* has been
27
28 obtained by using an integrated LC-MS and NMR metabolomics approach. Through integration
29
30 of resulting LC-MS and NMR metabolite profiles with previously published proteomics data, we
31
32 have been able to map several key metabolic pathways that seem to modulate *I. hospitalis-N*
33
34 *equitans* interspecies interactions. This study has highlighted key metabolic changes occurring
35
36 when *I. hospitalis* is grown in co-culture with *N. equitans*. Although *I. hospitalis* is able to grow
37
38 in the presence of *N. equitans*, our data suggests that there is a significant metabolic cost for the
39
40 host organism. *N. equitans* seems to consume a large fraction of the small molecule pool of *I.*
41
42 *hospitalis*, producing a sharp decrease in the energy status of the host. We cannot rule out that in
43
44 their natural environment, the interactions between these two organisms with severely reduced
45
46 genomes may confer an ecological advantage in the larger meta-microbial community, but the
47
48 results of this study suggest that, at least under the laboratory conditions used here, *N. equitans*
49
50 provides no adaptive advantage to *I. hospitalis* but rather imposes a significant metabolic energy
51
52 tax on *I. hospitalis*.
53
54
55
56
57
58
59
60
61
62
63
64
65

1
2
3
4 The combination of NMR and MS for untargeted metabolomics analysis has proven to be
5
6 very powerful and complementary. Often times, the two methods yielded similar metabolite
7
8 identification with comparable fold change measured by both for the different *I. hospitalis* and *I.*
9
10 *hospitalis* – *N. equitans* cultures. In some cases, metabolite identification was only possible using
11
12 either LC-MS or NMR but not both, making the use of both analytical platforms a necessity.
13
14
15 Furthermore, the additional sensitivity of LC-MS for low abundance molecules combined with
16
17 the ability of NMR to obtain quantitative metabolite concentrations (as opposed to relative
18
19 concentrations) demonstrate the highly advantageous application of both techniques to
20
21 untargeted metabolite profiling of microbial systems.
22
23
24
25
26
27
28
29
30
31
32
33
34
35
36
37
38
39
40
41
42
43
44
45
46
47
48
49
50
51
52
53
54
55
56
57
58
59
60
61
62
63
64
65

1
2
3
4 **References**
5

- 6
7 Boucher, Y., Kamekura, M., & Doolittle, W. F. (2004). Origins and evolution of isoprenoid lipid
8
9 biosynthesis in archaea. *Molecular Microbiology*, 52 (2), 515–527. doi:10.1111/j.1365-
10 2958.2004.03992.x
11
12
13
14 Burghardt, T., Junglas, B., Siedler, F., Wirth, R., Huber, H., & Rachel, R. (2009). The interaction
15
16 of *Nanoarchaeum equitans* with *Ignicoccus hospitalis*: proteins in the contact site between
17
18 two cells. *Biochemical Society Transactions*, 37, 127–32. doi:10.1042/BST0370127
19
20
21
22
23
24
25
26
27
28
29
30
31
32
33
34
35
36
37
38
39
40
41
42
43
44
45
46
47
48
49
50
51
52
53
54
55
56
57
58
59
60
61
62
63
64
65
- Chenomx NMR Suite 7.0. (2010). Chenomx Inc., Alberta, Canada.
- Giannone, R. J., Huber, H., Karpinets, T., Heimerl, T., Küper, U., Rachel, R., et al. (2011).
Proteomic characterization of cellular and molecular processes that enable the
Nanoarchaeum equitans--*Ignicoccus hospitalis* relationship. *PloS one*, 6(8), e22942.
doi:10.1371/journal.pone.0022942
- Godde, J. S. (2012). Breaking through a phylogenetic impasse: a pair of associated archaea might
have played host in the endosymbiotic origin of eukaryotes. *Cell & Bioscience*, 2(29), 1–11.
doi:10.1186/2045-3701-2-29
- Heinemann, J., Hamerly, T., Maaty, W. S., Movahed, N., Steffens, J. D., Reeves, B. D., et al.,
(2014). Expanding the paradigm of thiol redox in the thermophilic root of life. *Biochimica
et Biophysica Acta*, 1840(1), 80–85. doi:10.1016/j.bbagen.2013.08.009
- Huber, H., Burggraf, S., Mayer, T., Wyschkony, I., Rachel, R., & Stetter, K. O. (2000).
Ignicoccus gen. nov., a novel genus of hyperthermophilic, chemolithoautotrophic Archaea,
represented by two new species, *Ignicoccus islandicus* sp nov and *Ignicoccus pacificus* sp
nov. and *Ignicoccus pacificus* sp. nov. *International Journal of Systematic and Evolutionary*

1
2
3
4 Microbiology, 50, 2093–2100. Retrieved from

5
6 <http://www.ncbi.nlm.nih.gov/pubmed/11155984>

7
8
9 Huber, H., Gallenberger, M., Jahn, U., Eylert, E., Berg, I. a, Kockelkorn, D., et al., (2008). A
10
11 dicarboxylate/4-hydroxybutyrate autotrophic carbon assimilation cycle in the
12
13 hyperthermophilic Archaeum *Ignicoccus hospitalis*. Proceedings of the National Academy
14
15 of Sciences of the United States of America, 105(22), 7851–7856.
16
17
18 doi:10.1073/pnas.0801043105

19
20
21 Huber, H., Hohn, M. J., Rachel, R., Fuchs, T., Wimmer, V. C., & Stetter, K. O. (2002). A new
22
23 phylum of Archaea represented by a nanosized hyperthermophilic symbiont. Nature,
24
25 417(6884), 63–67. doi:10.1038/417063a

26
27
28 Huber, H., Hohn, M. J., Stetter, K. O., & Rachel, R. (2003). The phylum Nanoarchaeota: present
29
30 knowledge and future perspectives of a unique form of life. Research in Microbiology,
31
32 154(3), 165–171. doi:10.1016/S0923-2508(03)00035-4

33
34
35 Huber, H., Küper, U., Daxer, S., & Rachel, R. (2012). The unusual cell biology of the
36
37 hyperthermophilic Crenarchaeon *Ignicoccus hospitalis*. Antonie van Leeuwenhoek, 102,
38
39 203–219. doi:10.1007/s10482-012-9748-5

40
41
42
43 Jahn, U., Gallenberger, M., Paper, W., Junglas, B., Eisenreich, W., Stetter, K. O., et al., (2008).
44
45 *Nanoarchaeum equitans* and *Ignicoccus hospitalis*: new insights into a unique, intimate
46
47 association of two archaea. Journal of Bacteriology, 190(5), 1743–1750.
48
49
50 doi:10.1128/JB.01731-07

51
52
53 Jahn, U., Huber, H., Eisenreich, W., Hügler, M., & Fuchs, G. (2007). Insights into the
54
55 autotrophic CO₂ fixation pathway of the archaeon *Ignicoccus hospitalis*: comprehensive
56
57

1
2
3
4 analysis of the central carbon metabolism. *Journal of Bacteriology*, 189(11), 4108–4119.

5
6
7 doi:10.1128/JB.00047-07

8
9 Jahn, U., Summons, R., Sturt, H., Grosjean, E., & Huber, H. (2004). Composition of the lipids of
10
11 *Nanoarchaeum equitans* and their origin from its host *Ignicoccus* sp. strain KIN4/I.

12
13
14
15
16
17
18
19
20
21
22
23
24
25
26
27
28
29
30
31
32
33
34
35
36
37
38
39
40
41
42
43
44
45
46
47
48
49
50
51
52
53
54
55
56
57
58
59
60
61
62
63
64
65

Archives of Microbiology, 182, 404–413. doi:10.1007/s00203-004-0725-x

Junglas, B., Briegel, A., Burghardt, T., Walther, P., Wirth, R., Huber, H., & Rachel, R. (2008).

Ignicoccus hospitalis and *Nanoarchaeum equitans*: ultrastructure, cell-cell interaction, and
3D reconstruction from serial sections of freeze-substituted cells and by electron

cryotomography. *Archives of Microbiology*, 190, 395–408. doi:10.1007/s00203-008-0402-
6

Karp, P. D., Ouzounis, C. a, Moore-Kochlacs, C., Goldovsky, L., Kaipa, P., Ahrén, D., et al.,

(2005). Expansion of the BioCyc Collection of Pathway/Genome Databases to 160
Genomes. *Nucleic Acids Research*, 33(19), 6083–6089. doi:10.1093/nar/gki892

Karp, P. D., & Paley, S. (1996). Integrated Access to Metabolic and Genomic Data. *Journal of*

Computational Biology, 3(1), 191–212. Retrieved from

<http://www.ncbi.nlm.nih.gov/pubmed/8697237>

Karp, P. D., Paley, S. M., Krummenacker, M., Latendresse, M., Dale, J. M., Lee, T. J., et al.,

(2010). Pathway Tools version 13.0: Integrated Software for Pathway/Genome Informatics
and Systems Biology. *Briefings In Bioinformatics*, 11(1), 40–79. doi:10.1093/bib/bbp043

Karp, P. D., Paley, S., & Romero, P. (2002). The Pathway Tools Software. *Bioinformatics*, 18,

S1–8.

Küper, U., Meyer, C., Müller, V., Rachel, R., & Huber, H. (2010). Energized outer membrane

and spatial separation of metabolic processes in the hyperthermophilic Archaeon *Ignicoccus*

1
2
3
4 *hospitalis*. Proceedings of the National Academy of Sciences of the United States of
5
6
7 America, 107(7), 3152–3156. doi:10.1073/pnas.0911711107
8
9 Moran, U., Phillips, R., & Milo, R. (2010). SnapShot: key numbers in biology. Cell, 141(7),
10
11 1262–1262.e1. doi:10.1016/j.cell.2010.06.019
12
13
14 Paley, S. M., Latendresse, M., & Karp, P. D. (2012). Regulatory network operations in the
15
16 Pathway Tools software. BMC Bioinformatics, 13, 243. doi:10.1186/1471-2105-13-243
17
18
19 Paper, W., Jahn, U., Hohn, M. J., Kronner, M., Näther, D. J., Burghardt, T., et al., (2007).
20
21 *Ignicoccus hospitalis* sp. nov., the host of “*Nanoarchaeum equitans*”. International Journal
22
23 of Systematic and Evolutionary Microbiology, 57, 803–808. doi:10.1099/ijs.0.64721-0
24
25
26 Podar, M., Anderson, I., Makarova, K. S., Elkins, J. G., Ivanova, N., Wall, M. A., et al., (2008).
27
28 A genomic analysis of the archaeal system *Ignicoccus hospitalis*-*Nanoarchaeum equitans*.
29
30 Genome Biology, 9, R158. doi:10.1186/gb-2008-9-11-r158
31
32
33 Promega Corporation. (2012). BacTiter-Glo Microbial Cell Viability Assay.
34
35
36 Sun, J., Zhang, S., Chen, J., & Han, B. (2012). Metabolic profiling of *Staphylococcus aureus*
37
38 cultivated under aerobic and anaerobic conditions with ¹H NMR-based nontargeted
39
40 analysis. Canadian Journal of Microbiology, 718(17), 709–718. doi:10.1139/W2012-046
41
42
43 Tredwell, G. D., Edwards-Jones, B., Leak, D. J., & Bundy, J. G. (2011). The development of
44
45 metabolomic sampling procedures for *Pichia pastoris*, and baseline metabolome data. PloS
46
47 one, 6(1), e16286. doi:10.1371/journal.pone.0016286
48
49
50 Waters, E., Hohn, M. J., Ahel, I., Graham, D. E., Adams, M. D., Barnstead, M., et al., (2003).
51
52 The genome of *Nanoarchaeum equitans*: insights into early archaeal evolution and derived
53
54 parasitism. Proceedings of the National Academy of Sciences of the United States of
55
56 America, 100(22), 12984–12988. doi:10.1073/pnas.1735403100
57
58
59
60
61
62
63
64
65

1
2
3
4
5
6
7
8
9
10
11
12
13
14
15
16
17
18
19
20
21
22
23
24
25
26
27
28
29
30
31
32
33
34
35
36
37
38
39
40
41
42
43
44
45
46
47
48
49
50
51
52
53
54
55
56
57
58
59
60
61
62
63
64
65

Weljie, A. M., Newton, J., Mercier, P., Carlson, E., & Slupsky, C. M. (2006). Targeted profiling: quantitative analysis of ¹H NMR metabolomics data. *Analytical Chemistry*, 78(13), 4430–4442. doi:10.1021/ac060209g

Wishart, D. S. (2008). Quantitative metabolomics using NMR. *Trends in Analytical Chemistry*, 27(3), 228–237. doi:10.1016/j.trac.2007.12.001

Wu, X.-H., Yu, H.-L., Ba, Z.-Y., Chen, J.-Y., And, H.-G. S., & Han, B.-Z. (2010). Sampling methods for NMR-based metabolomics of *Staphylococcus aureus*. *Biotechnology Journal*, 5(1), 75–84.

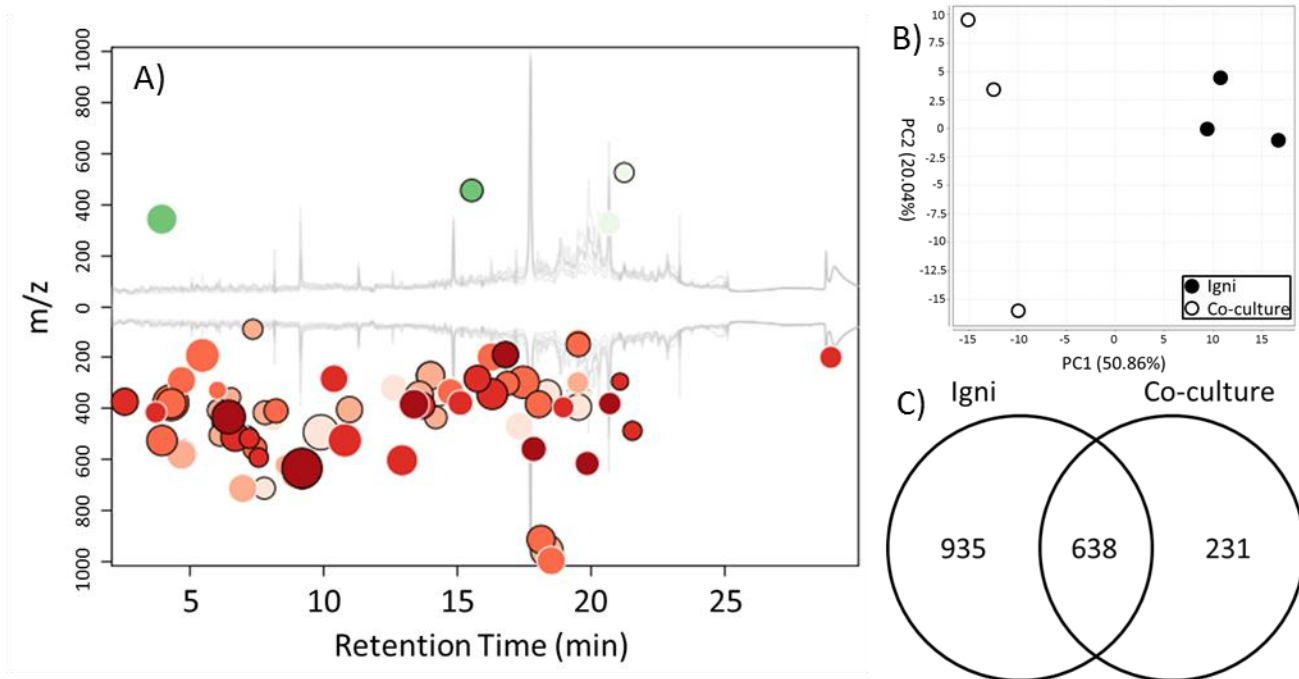


Figure. 1 Analysis of metabolites by RP LC-MS

(A) Cloud plot of extracted metabolites from *I. hospitalis* grown alone top, and co-culture of *I. hospitalis* and *N. equitans* bottom. Green circles denote a chromatographic peak whose mass spectral (MS) molecular feature is more abundant in the co-culture, and red circles denote a peak whose MS molecular feature is more abundant in *I. hospitalis* grown alone. The x-axis displays the retention/elution time of each molecular feature, while the y-axis indicates the m/z for each molecular feature. Only molecular features with a fold change greater than 1.5 and a p-value less than 0.01 are shown. (B) A 2D PCA score plot indicating the separation of biological triplicates for *I. hospitalis* and the *I. hospitalis-N. equitans* co-culture. The co-culture exhibits more variance in PC2 than the *I. hospitalis* samples; this likely arises from the variability that *N. equitans* contributes when grown with *I. hospitalis*. (C) Venn diagram indicating the number of unique and shared MS molecular features found in each sample.

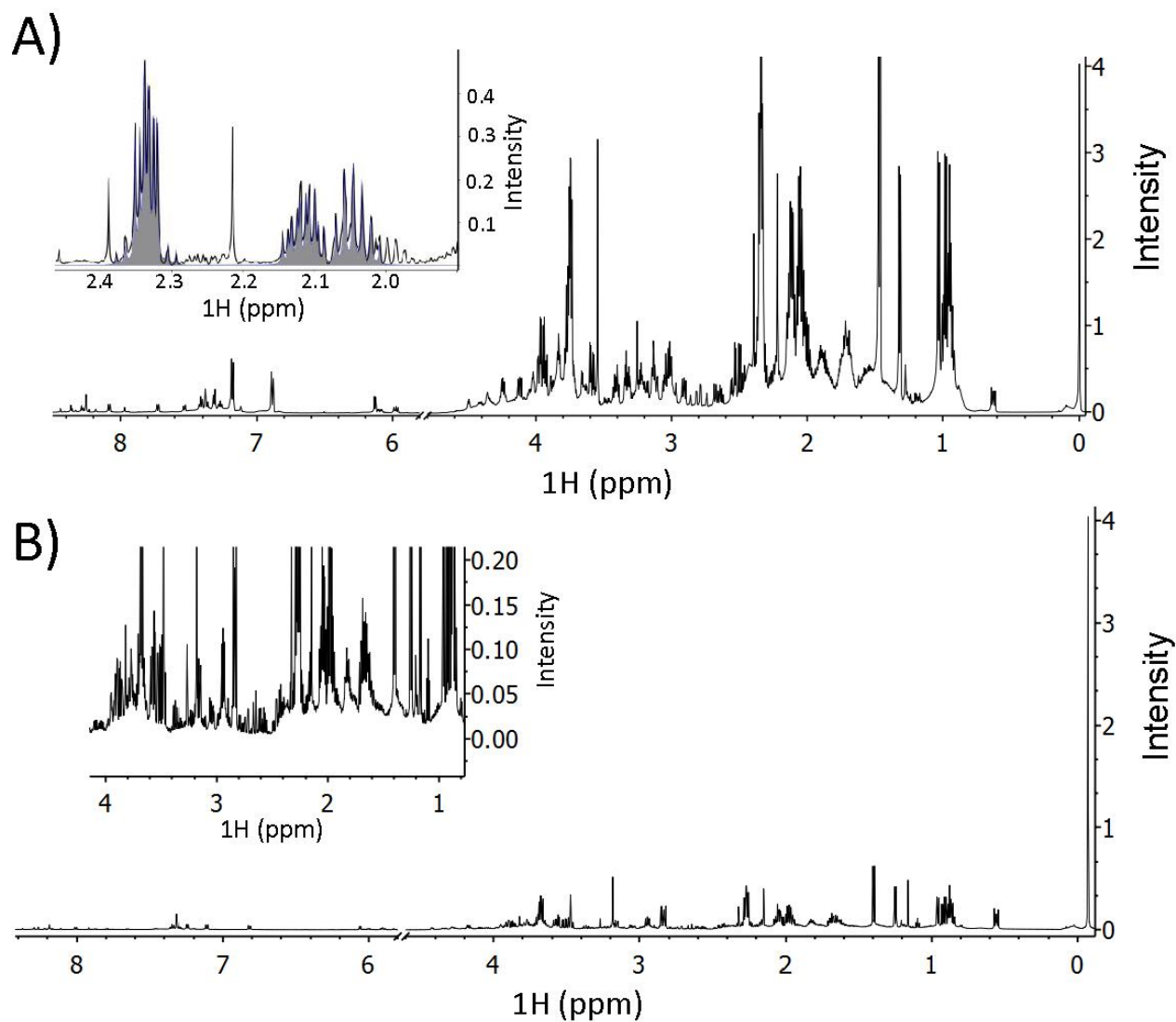


Figure. 2 1D ^1H NMR spectra of *I. hospitalis* and *N. equitans* intracellular metabolite profiles

1D ^1H NMR spectra of **(A)** *I. hospitalis* only culture and **(B)** the *I. hospitalis*–*N. equitans* co-culture, highlighting differences in overall metabolite concentrations and their overall depletion in the *I. hospitalis*–*N. equitans* co-culture samples. The insert in panel A highlights the spectral fitting (in blue) of NMR resonances corresponding to glucose. In panel B, the inserts presents a zoomed in spectral region of the ^1H 1D spectrum of an *I. hospitalis*–*N. equitans* co-culture sample, spanning the ^1H chemical shift range of 0 to 5 ppm.

Figure 3
[Click here to download Figure: Fig3_Igni_Nano.pptx](#)

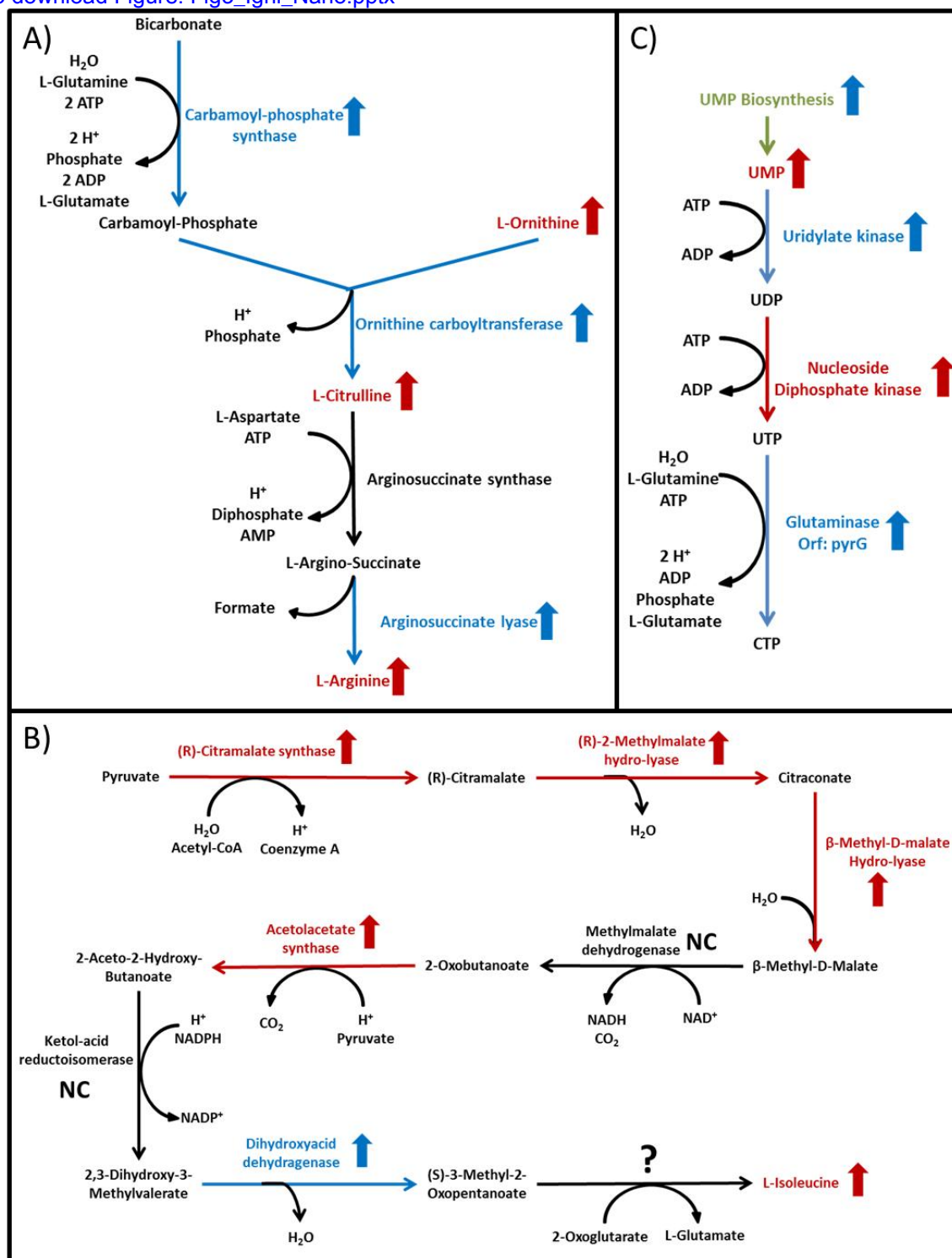


Figure. 3 Pathway Analysis

Overlay of proteomic and metabolomic analysis for three metabolic pathways: arginine biosynthesis (A), isoleucine biosynthesis (B), and CTP Biosynthesis (C). Proteins and metabolites identified by proteomics and metabolomics experiments which displayed a fold change greater than 1.5 between cultures are highlighted in color; red indicates a greater concentration in the *I. hospitalis* only culture, while blue indicates a greater concentration in the *I. hospitalis*-*N. equitans* co-culture.

Table 1 Table 1. Metabolites identified by LCMS and NMR
[Click here to download Table: Table 1 \(final\).pptx](#)

LC-MS	Pwy	Std	Fold	p-value	NMR	Fold
(3S)-3,6-Diaminohexanoate	X		4.63	0.2378	2-Aminoadipate	3.27
2-Oxo-4-Methylthiobutanoate	X		*	-	2-Oxoisocaproate	#
5-Oxoproline	X		2.70	0.0776	3-Methyl-2-oxovalerate	#
Adenine	X		*	-	5,6-Dihydrothymine	*
AMP		X	8.79	0.0725	Adenosine	-1.34
Agmatine	X	X	2.76	0.2173	ADP	1.72
Butanal	X		-1.40	0.5231	Agmatine	*
CMP		X	3.24	0.1898	AMP	6.81
Glucuronamide		X	#	-	Betaine	1.17
Hydroxymethylbilane	X		#	-	Carnitine	#
L-2-Aminoadipate	X		4.38	0.0686	Cytidine	-2.72
L-Arginine	X	X	1.78	0.2986	Dimethyl sulfone	38.13
L-Aspartate	X	X	2.38	0.5679	Dimethylamine	53.21
L-Aspartyl-4-Phosphate	X		#	-	dTTP	1.09
L-Citrulline	X	X	3.62	0.1227	Formate	1.61
L-Glutamate	X	X	2.28	0.1205	Fumarate	*
L-Histidine	X	X	24.75	0.3924	Glucose	#
L-Homoserine	X	X	6.93	0.0057	Glycine	10.21
L-Isoleucine	X	X	1.93	0.3817	Guanosine	#
L-Leucine	X	X	1.93	0.3817	Indole-3-acetate	1.80
L-Lysine	X	X	4.63	0.2378	Inosine	2.12
L-Phenylalanine	X		-1.04	0.9092	Lactate	2.25
L-Proline	X	X	5.34	0.0074	L-Alanine	11.16
L-Threonine	X	X	6.93	0.0057	L-Arginine	3.00
Maltotriose		X	#	-	L-Asparagine	#
Menadione	X		2.39	0.0902	L-Aspartate	13.67
N2-Acetyl-L-Lysine	X		5.55	0.0275	L-Citrulline	11.94
N-Acetyl-L-Glutamate	X	X	6.45	0.0095	L-Glutamate	9.20
O-Acetyl-L-Homoserine	X		4.38	0.0686	L-Histidine	6.37
O-Succinyl-L-Homoserine	X		*	-	L-Isoleucine	3.40
Phenylethyl-amine		X	1.10	0.5097	L-Leucine	4.88
Phytyl Diphosphate	X		#	-	L-Lysine	3.44
Propanal	X		-1.37	0.6935	L-Methionine	7.45
Pseudouridine 5'-Phosphate	X		*	-	L-Ornithine	15.75
Riboflavin	X		7.91	0.0592	L-Phenylalanine	1.96
S-Adenosyl-L-Homocysteine	X		*	-	L-Proline	28.25
Stachyose		X	#	-	L-Pyroglutamate	#
Tyramine		X	1.08	0.2693	L-Serine	10.19
Tyrosol	X		1.50	0.1537	L-Threonine	5.94

- Putatively metabolite IDs based on annotated pathways from Biocyc (**Pwy**)
- Confirmed metabolite IDs based on MS standards (**Std**)
- Metabolite IDs from spectral features of compounds identified by NMR (**NMR**)
- Fold change between the *I. hospitalis* only samples and the *I. hospitalis* – *N. equitans* co-culture, where a positive number indicates a higher concentration in the *I. hospitalis* only culture.
- * denotes a compound seen only in the *I. hospitalis* culture
- # denotes a compound seen only when *N. equitans* is present in the co-culture.

L-Tryptophan	6.13
L-Tyrosine	7.84
L-Valine	6.06
Malonate	6.38
N-Acetyltyrosine	*
Nicotinate	1.16
N-Isovaleroylglycine	#
Oxypurinol	#
S-Adenosylhomocysteine	2.79
Succinate	7.58
Trehalose	-1.65
UDP-glucose	1.80
UDP-N-Acetylglucosamine	1.39
UMP	2.39
Uracil	-1.65
Uridine	-1.48